Large Eddy Simulations of the turbulent katabatic flow developing along a hyperbolic tangent slope in stable atmospheric boundary layer

Christophe Brun, Jean-Pierre Chollet

LARGE EDDY SIMULATION OF THE TURBULENT KATABATIC FLOW DEVELOPING ALONG A HYPERBOLIC TANGENT SLOPE IN STABLE ATMOSPHERIC BOUNDARY LAYER.

Christophe Brun
Laboratoire des Ecoulements Géophysiques et Industriels,
Université J. Fourier, 38000 Grenoble, France
christophe.brun@hmg.inpg.fr

Jean-Pierre Chollet
Laboratoire des Ecoulements Géophysiques et Industriels,
Université J. Fourier, 38000 Grenoble, France
jean-pierre.chollet@ujf-grenoble.fr

ABSTRACT

Large Eddy Simulations of the turbulent katabatic flow developing along a hyperbolic tangent slope are performed in the context of stable atmospheric boundary layer. The effects of ground surface boundary conditions and initial temperature stratification are analysed. It is shown that, even for stratification up to $N = 0.020\ s^{-1}$, that is to say the upper limit for on site measurements, turbulent structures develop and turbulent heat fluxes and turbulent shear stresses increase in the downslope jet close to the ground surface. Mixing might be increased, a property of direct importance for pollution prediction.

INTRODUCTION

The understanding and the prediction of turbulent atmospheric flows along alpine valleys is of many practical interest related to meteorology and air pollution prediction [16, 3]. The night-day thermodynamic cycle is a key constraint for the flow development. During the night period, the air is often stably stratified and the cold ground generates a negative heat flux which yields a katabatic flow along the slope in direction to the valley, due to gravity effect [6, 7, 15]. Such flow contributes to concentrate pollutants in the valley and therefore is important to analyse and model as precisely as possible.

The purpose of the present numerical study is to artificially generate a katabatic flow along a very simple model of valley slope submitted to a negative heat flux at the wall. As a starting point, we consider a stably stratified fluid at rest. Such configuration is particularly difficult to simulate in comparison to neutral and convective atmospheric boundary layers (ABL) [13, 17, 10] and is now being possibly tackled thanks of the development of high performance computers allowing for highly resolved simulations [14, 1, 18, 19, 8, 5, 4, 11]. Large Eddy Simulation of the turbulent stable ABL along a slope is presently considered to assess two complementary issues:

(i) the statistical quantitative characterisation of katabatic flow driven by momentum and temperature wall shear stresses under stable stratification.

(ii) the qualitative description of turbulent structures developing in the outer part of the ABL subjected to a strong shear.

FLOW CONFIGURATION AND NUMERICAL ASPECTS

The numerical code Meso-NH presently used for the simulation has been developed in CNRM/Météo-France and Laboratoire d'Aérologie Toulouse [2]. It consists of a non-hydrostatic model solving the pseudo-incompressible Navier-Stokes equations written in a conservative form with an anelastic approximation introduced by Duran in 1989 [9]. Dry air is considered as a perfect gas and buoyancy effects are introduced in the momentum equation while Coriolis rotation effects are neglected.

Since ABL are highly turbulent flows, Large Eddy Simulation (LES) is considered with an extra transport equation for the sub-grid scale kinetic energy in complement to momentum and potential temperature equations, coupled with a mixing length closure for the determination of the turbulent stresses. Numerical discretisation is performed with 4^{th} order centred scheme for the momentum equation, 2^{nd} order centred positive definite scheme for the temperature and kinetic energy equations, and the pressure solver consists of a Conjugate Residual method.

The numerical domain of simulation consists of a large 3D domain of height L_z, length L_x and width L_y on the top of a 2D hyperbolic tangent slope with a height H and a maximum angle α_{max}, to represent a simple model of alpine valley (Table 1). About 5 million grid points are necessary to afford a relatively precise description of the flow in the vicinity of the wall, with a special refinement in the vertical direction to capture the wall jet developing along the slope. The time step of the simulation is about $\Delta t = 0.05s$ that is to say $4s$ CPU on 8 processors of the Nec Sx-8 french high-performance computer (IDRIS).

$L_x(m)$	$L_y(m)$	$L_z\ (m)$	n_x	n_y	n_z
$3,200$	$1,280$	$7,250$	128	128	300
Δx	Δy	Δz_{wall}	Δz_{top}	$H\ (m)$	α_{max}
$25\ m$	$10\ m$	$1\ m$	$120\ m$	$1,000$	35.5^o

Table 1: Domain configuration

The setting of initial and boundary conditions is crucial for the simulation of stable ABL. Initial conditions consist of air at rest following a stably stratified temperature profile with a constant Brunt-Väisälä frequency $N = 0.013\ s^{-1}$ (cases R0Q3N13, U0Q3N13 and U0Q1N13), $N = 0.007\ s^{-1}$ (case U0Q3N07), $N = 0.020\ s^{-1}$ (case U0Q3N20). Periodic-

ity is considered in the spanwise L_y direction of the domain. Open Orlanski type boundary conditions are applied in the slope L_x direction of the ABL, with an advection velocity set to $u_x(n_x) + c$, $u_x(n_x)$ being the streamwise velocity at the boundary and $c = 10\ m/s$ a phase velocity of the order of magnitude of the gravity waves expected to spread in such configuration. On the top of the domain, non-reflective boundary conditions are considered. At the wall, the minimum vertical mesh size $\Delta z_{wall} = 1\ m$ is of the order of the boundary layer thickness. At the surface two sets of boundary conditions have been considered (Table 2), first a rough surface condition with a roughness lengthscale $z_o = 3.5\ cm$ (case R0Q3N13)[4], second ideal cases with free slip conditions inducing a zero surface shear stress $\tau_w = 0$ (cases U0Q3N13, U0Q3N07, U0Q3N20, U0Q1N13). The boundary condition at the ground surface for the thermal field is a constant negative heat flux $q_w = -30\ W/m^2$ [18, 19] for the cases R0Q3N13, U0Q3N13, U0Q3N07, U0Q3N20 and $q_w = -10\ W/m^2$ for the case U0Q1N13.

Case	r_o / u_τ	$q_w\ (W/m^2)$	$N(s^{-1})$	U_{max}
R0Q3N13	0.35 m	-30	0.013	1.5 m/s
U0Q3N13	0. m/s	-30	0.013	2.7 m/s
U0Q1N13	0. m/s	-10	0.013	1.6 m/s
U0Q3N07	0. m/s	-30	0.007	4.0 m/s
U0Q3N20	0. m/s	-30	0.020	2.2 m/s

Table 2: Flow configuration

MAIN RESULTS

Fluid is initially at rest under stable stratification $0.007s^{-1} \leq N = \left(\frac{g}{\theta_o}\frac{\partial\theta}{\partial z}\right)^{0.5} \leq 0.020s^{-1}$. The case U0Q3N07 ($N = 0.007s^{-1}$) is close to a neutral condition ($N = 0s^{-1}$) such as the one reported in [18, 19]. In this sense, the present simulations are performed with more intense stratification conditions which might somehow prevent turbulence to spread in the vertical direction. Cooling at the ground surface ($q_w \leq 0.$) is applied and yields a surface deficit of mean potential temperature of about 1 to 4 K (fig. 1). The combination of gravity effects along the surface slope generates a katabatic down-slope flow with all the classical trends [6, 7, 18, 19, 4, 5]. After a transient of about 30 minutes for all cases presently reported, the flow reaches a mean equilibrium state which consists of a low-level down-slope jet with a maximum mean streamwise velocity in the range $1m/s \leq U_{max} \leq 4m/s$ (Table 2) and a width of about 10 to 30 m (fig. 2). While the qualitative behaviour of the flow is similar for all cases, the computed velocity and lengthscales of the flow are strongly sensitive to initial N conditions and surface q_w and τ_w boundary conditions. First, we note that the higher the initial stratification, the lower the maximum jet velocity. Second, the use of a rough surface is necessary to describe the bulk jet shape while free slip boundary conditions yields a nearly twice thinner jet width. This second choice is nevertheless efficient to freely describe the downslope velocity for the present high Reynolds number flow for which the full boundary layer description is computationally presently not affordable.

The main dynamics of the flow is concentrated in the first 100 m of the ABL while the top of the domain is kept at the bottom of the troposphere at about 7000 m to allow for further investigations related to geophysical aspects such as gravity wave description. The precise description of the ABL is expected to play a key role in the wave generation or wave interaction in the external region of the ABL. In such context, the present study aims at describing the turbulent properties of the katabatic flow and especially the external shear region of the downslope jet. After the flow has reached a fully turbulent regime, a strong mean shear is observed in the external part of the ABL all along the slope (fig. 2) where kinetic energy is produced (not shown). Figures (3) and (4) show the vertical profiles for the resulting turbulent shear stress and turbulent heat flux, respectively. Maximum is obtained in the region between 10 to 20 m, dependent on boundary and initial conditions. But, the amplitude of the profiles is not directly linked to the quantitative fluxes applied as boundary conditions, which confirms the separation process produced by the downslope jet between the two inner and outer-layer regions already observed in [4, 5]. Furthermore, the effect of temperature stratification is not straightforward since it can be seen that for increasing N turbulent stresses and turbulent heat fluxes do not necessarily decrease.

Visualisations of the Q-criterion are shown on figures (5) and (6). For all cases, transition to turbulence occurs in the shear layer zone and turbulent structures develop, are stretched and might be advected further down the slope. While the initial mechanism of vortex formation is related to Kelvin-Helmholtz instability (not shown), vortices are rapidly stretched in the streamwise direction and elongated Görtler like turbulent structures develop (figs. 5 and 6) as a possible result of the surface curvature [12]. The isovalue of Q has been set based on an estimation of the global centrifugal effect of the present configuration about $\langle u\rangle^2/R^2 = 10^{-5}\ s^{-2}$ (R being the TH slope curvature), which confirms the present interpretation. These turbulent structures develop in regions where the mean local gradient Richardson number $Ri = N(z)^2/\frac{\partial u}{\partial z}^2$ is lower than the critical value $Ri_c = 0.25$ [16]. In the present computations, all cases are concerned in a layer of about 5 to 20 m in the ABL (fig. 7), where both velocity and potential temperature profiles are strongly distorted. For $N = 0.007s^{-1}$, turbulent structures are concentrated in the bottom region downstream the slope, while for $N = 0.020s^{-1}$ they spread up to the origin of the katabatic flow upstream. For all cases, this regions are fully correlated with isosurfaces of $Ri = 0.25$ (figs. 5 and 6). This shows that initial stable conditions are strongly modified by the development of the katabatic flow which behaves indeed as an important source of turbulence at the ground surface and increase local mixing. In the present configuration, curvature effects promote mixing as well since contrarotating streamwise vortices might eject flow and heat from the surface towards the atmosphere. In further work, curvature Richardson number (Bradshaw 1969) will be determined and the relation between Görtler instability and stable stratification will be discussed. Finally we note that the two cases U0Q1N13 and U0Q3N20 show very similar results both for normalised statistics profiles and instantaneous turbulent structure visualisations, while they correspond to changes in both wall heat flux boundary condition and initial temperature stratification. This confirms that they are two main ingredients to account for when seeking a universal behaviour of such a turbulent flow.

CONCLUSION

LES of the katabatic flow developing along a hyperbolic tangent slope has been performed with a special focus on the turbulent surface downslope jet generated by surface cool-

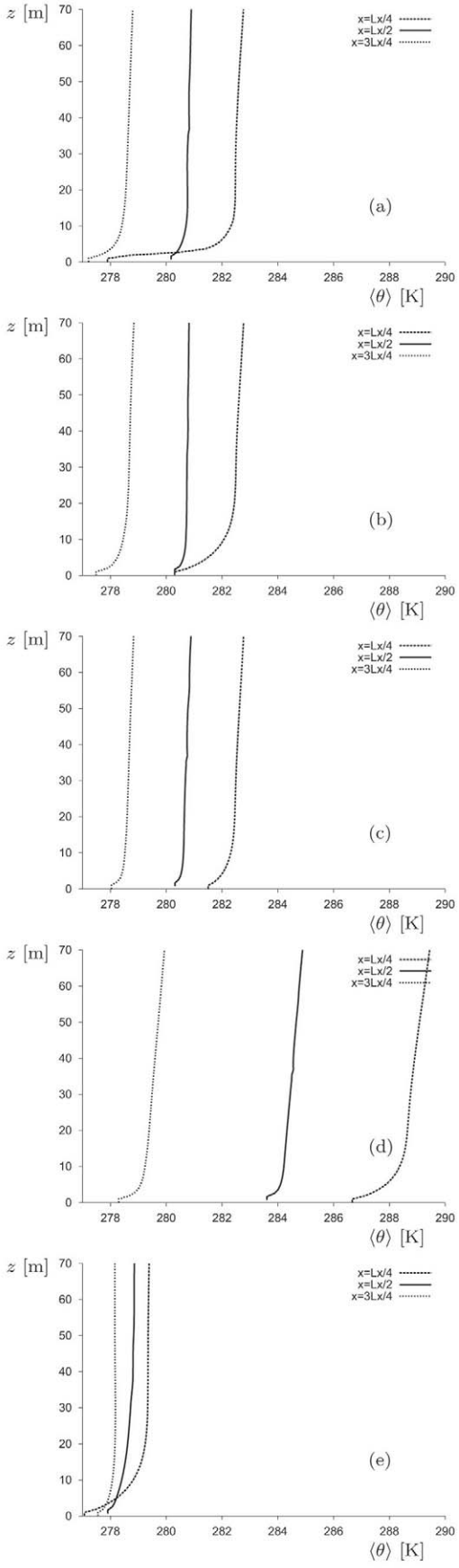

Figure 1: Mean potential temperature profiles at 3 stations along the TH slope, $x_1 = L_x/4$, $x_2 = L_x/2$ and $x_3 = 3L_x/4$. Reference case $N = 0.013s^{-1}$, roughness $r_o = 0.35\ m$, $q_w = -30\ W/m^2$ (a). Change in $u_\tau = 0$ (b). Change in $q_w = -10\ W/m^2$ (c). Change in $N = 0.020s^{-1}$ (d) and $N = 0.007s^{-1}$ (e).

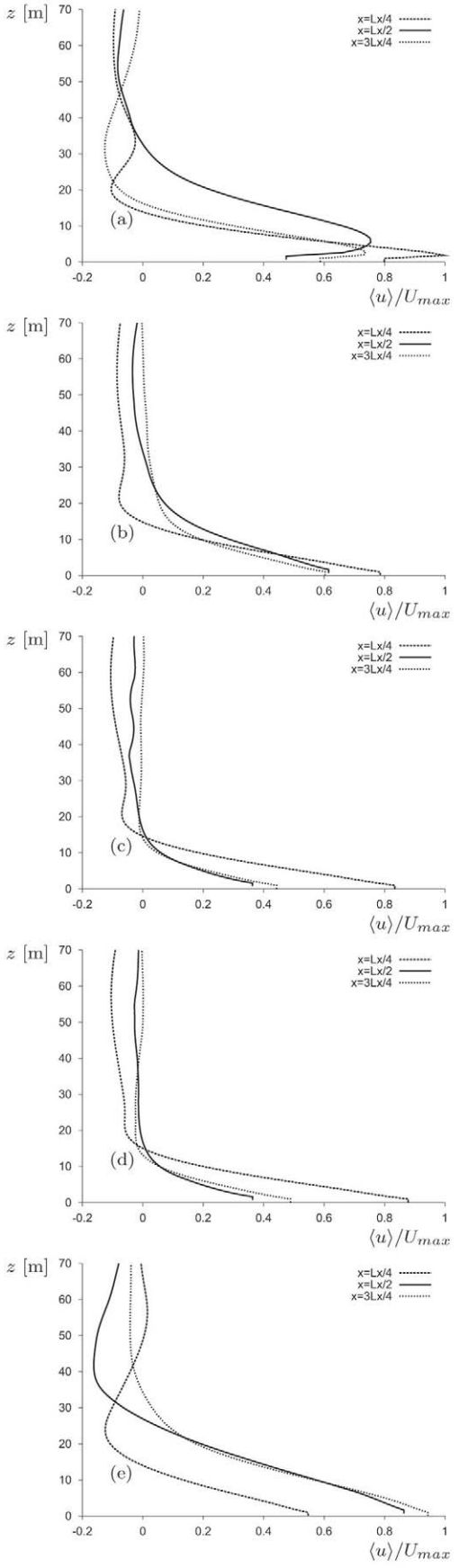

Figure 2: Mean stream-wise velocity profiles at 3 stations along the TH slope, $x_1 = L_x/4$, $x_2 = L_x/2$ and $x_3 = 3L_x/4$. Reference case $N = 0.013s^{-1}$, roughness $r_o = 0.35\ m$, $q_w = -30\ W/m^2$ (a). Change in $u_\tau = 0$ (b). Change in $q_w = -10\ W/m^2$ (c). Change in $N = 0.020s^{-1}$ (d) and $N = 0.007s^{-1}$ (e).

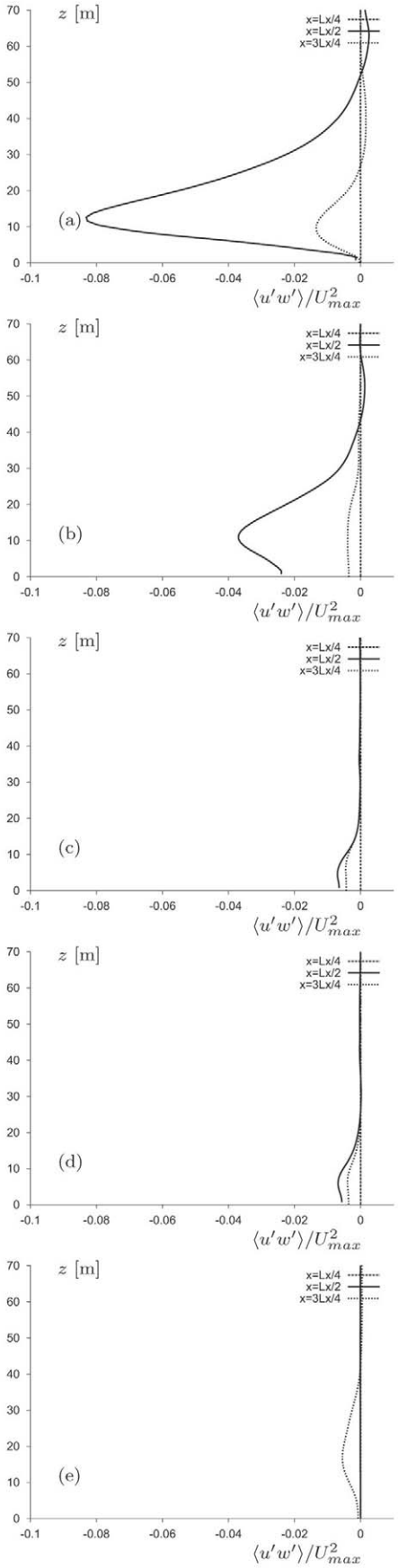

Figure 3: Turbulent stresses profiles at 3 stations along the TH slope, $x_1 = L_x/4$, $x_2 = L_x/2$ and $x_3 = 3L_x/4$. Reference case $N = 0.013s^{-1}$, roughness $r_o = 0.35\ m$, $q_w = -30\ W/m^2$ (a). Change in $u_\tau = 0$ (b). Change in $q_w = -10\ W/m^2$ (c). Change in $N = 0.020s^{-1}$ (d) and $N = 0.007s^{-1}$ (e).

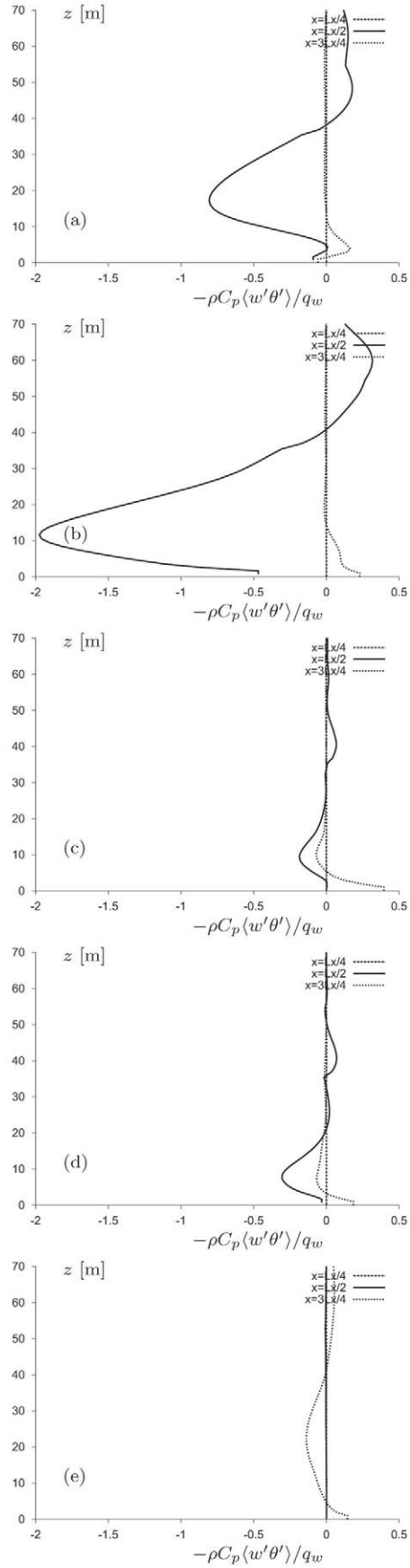

Figure 4: Turbulent heat flux profiles at 3 stations along the TH slope, $x_1 = L_x/4$, $x_2 = L_x/2$ and $x_3 = 3L_x/4$. Reference case $N = 0.013s^{-1}$, roughness $r_o = 0.35\ m$, $q_w = -30\ W/m^2$ (a). Change in $u_\tau = 0$ (b). Change in $q_w = -10\ W/m^2$ (c). Change in $N = 0.020s^{-1}$ (d) and $N = 0.007s^{-1}$ (e).

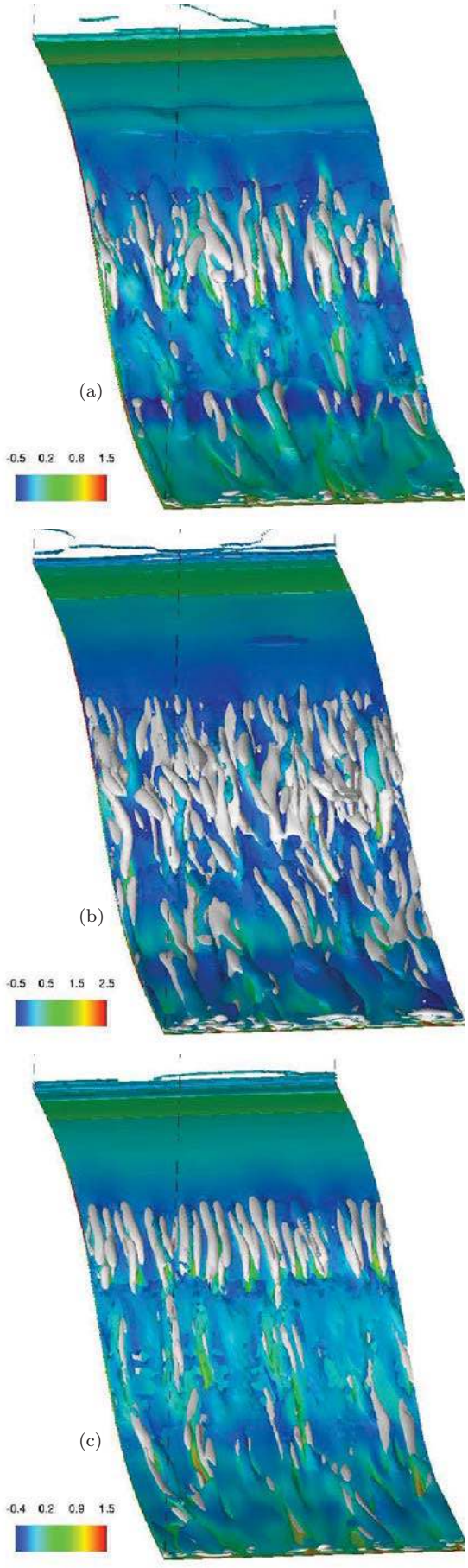

Figure 5: Isovalues of the Q criterion $Q = 10^{-5}s^{-2}$ (grey) and Richardson number $Ri = 0.25$ (colored by the streamwise velocity [m/s]), in the external shear layer of the ABL. Cases R0Q3N13 (a) , U0Q3N13 (b) and U0Q1N13 (c).

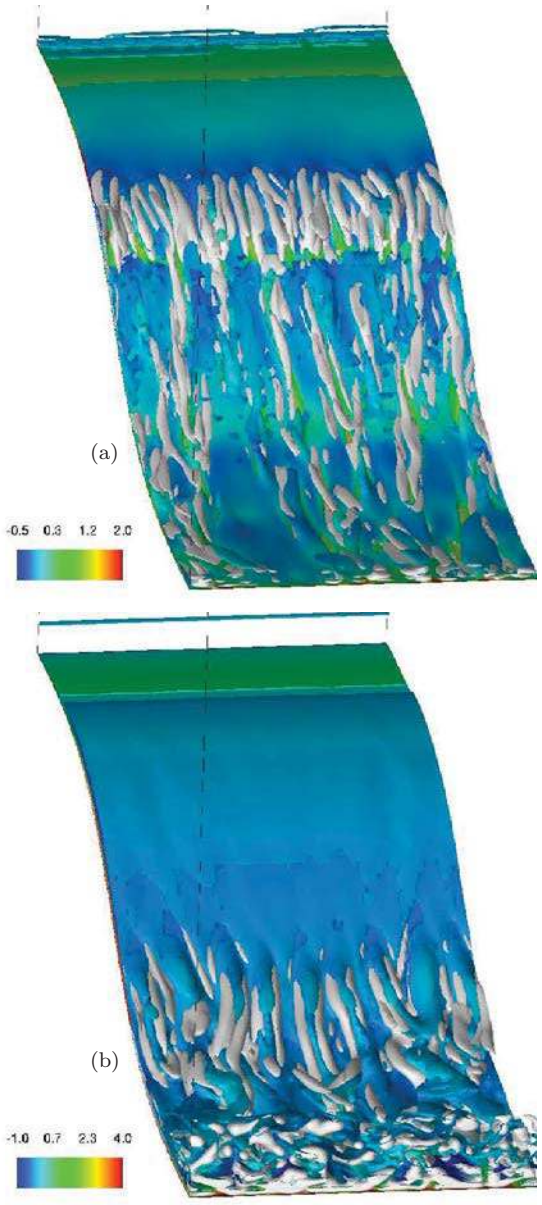

Figure 6: Isovalues of the Q criterion $Q = 10^{-5}s^{-2}$ (grey) and Richardson number $Ri = 0.25$ (colored by the streamwise velocity [m/s]), in the external shear layer of the ABL. Cases U0Q3N20 (a) and U0Q3N07 (b).

ing. Analysis based on turbulent statistics and turbulent structure visualisations show the impact of surface boundary conditions including surface roughness and surface heat flux, initial temperature stratification and orography curvature. While stable stratification is expected to inhibit turbulence transition, the present flow configuration shows that katabatic flows are good candidates to promote local mixing and thus are of interest for air quality prediction. A special result concerns the shape of the ground surface which plays an important role in the process of turbulence enhancement, an issue which has been already addressed, *e.g.* in the following terms: *'In a concave, unstable region an inviscid instability mechanism promotes the growth of streamwise vortices similar to the Görtler vortices of laminar flow and scalar transfer is greatly increased'* (Kaimal and Finnigan 1994) [12].

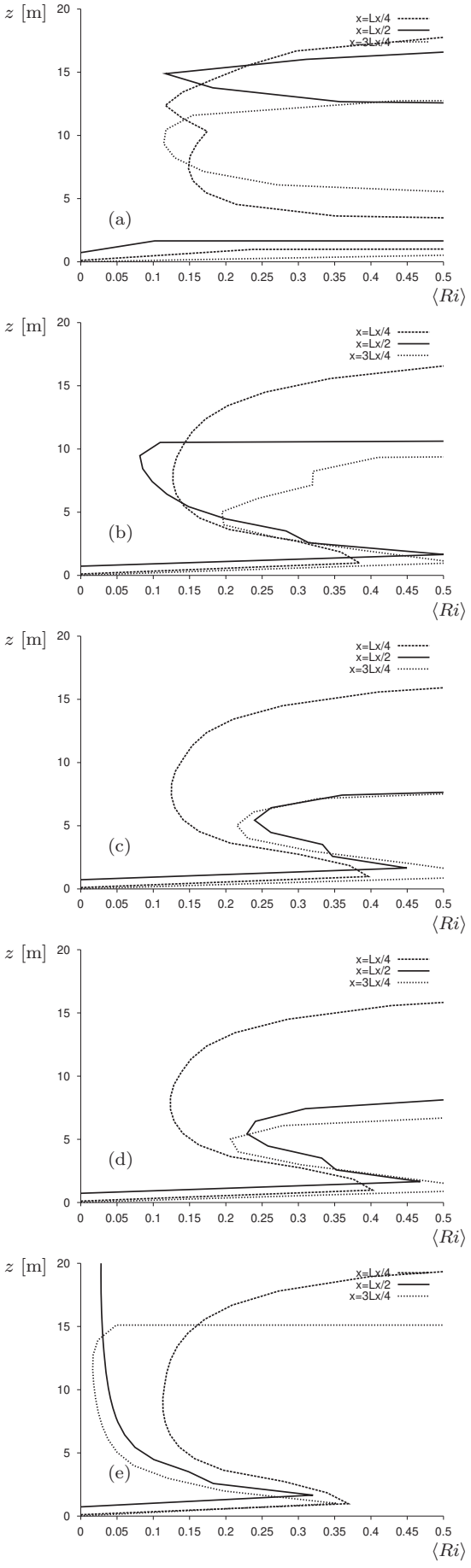

Figure 7: Profiles of the mean gradient Richardson number at 3 stations along the TH slope, $x_1 = L_x/4$, $x_2 = L_x/2$ and $x_3 = 3L_x/4$. Reference case $N = 0.013s^{-1}$, roughness $r_o = 0.35\ m$, $Q_w = -30\ W/m^2$ (a). Change in $u_\tau = 0$ (b). Change in $Q_w = -10\ W/m^2$ (c). Change in $N = 0.020s^{-1}$ (d) and $N = 0.007s^{-1}$ (e).

*

References

[1] A. Andren. The structure of stably stratified atmospheric boundary layers: a large-eddy simulation study. *Quart. J. Roy. Meteor. Soc.*, 121:961–985, 1995.

[2] P. Bougeault, P. Mascart, and J.P. Chaboureau. The meso-nh atmospheric simulation system: Scientific documentation. Météo-France, CNRS, 2008. http://mesonh.aero.obs-mip.fr/mesonh/.

[3] J.P. Chollet, Y. Largeron, and C Staquet. Modelling urban area in alpine complex terrain in winter time. In *13th Conference on Mountain Meteorology*, 2008. Whistler, BC, Canada.

[4] J. Cuxart and M.A. Jimenez. Mixing processes in a nocturnal low-level jet: an les study. *J. of the atmospheric sciences*, 59(17):2513–2534, 2006.

[5] J. Cuxart, M.A. Jimenez, and D. Martinez. Nocturnal meso-beta basin and katabatic flows on a mildaltitude island. *Monthly Weath. Rev.*, 135:919–932, 2006.

[6] J.C. Doran and T.W. Horst. Observations and models of simple nocturnal flows. *J. of the atmospheric sciences*, 40:708–717, 1983.

[7] J.C. Doran and T.W. Horst. The developement and structure of nocturnal slope winds in a simple valley. *Boundary-layer Meteorol.*, 52:41–68, 1990.

[8] P. Drobrinski. Dynamique de la couche limite atmosphérique: de la turbulence aux systèmes de méso-echelle. In *HDR Thesis*, 2005. Université Paris VI.

[9] D.R. Duran. Improving the anelastic approximation. *J. Atmo. Sci.*, 46:1453–1461, 1989.

[10] E. Federovich and Conzemius R. Large-eddy simulation of convective entrainment in linearly and discretely stratified fluids. In B.J. Geurts, R. Friedrich, and O. (eds.) Métais, editors, *Direct and Large-Eddy Simulation IV*, pages 299–310, Dordrecht, 2001. Kluwer Academic Publishers.

[11] C. Higgins, M. Parlange, C. Meneveau, E. Bou-Zeid, V. Kumar, and S. Chester. Les and related techniques: simulations in the atmospheric boundary layer. In *VKI lecture series 2008-4*, 2008.

[12] J.C. Kaimal and J.J. Finnigan. *Atmospheric boundary layer flows : their structure and measurement*. Oxford University Press US, 1994. ISBN 0195062396.

[13] P.J. Mason. Large-eddy simulation of the convective atmospheric boundary layer. *J. of the atmospheric sciences*, 46(11):1492–1516, 1988.

[14] P.J. Mason and D.J. Derbyshire. Large-eddy simulation of the stably stratified atmospheric boundary layer. *Boundary-layer meteorology*, 53:117–162, 1990.

[15] P. Monti, H.J.S. Fernando, M. Princevac, W.C. Chan, T.A. Kowalewski, and E.R. Pardyjak. Observations of flow and turbulence in the nocturnal boundary layer over a slope. *J. of the atmospheric sciences*, 59(17):2513–2534, 2002.

[16] F.T.M. Nieuwstadt and Meeder J.P. Les of air pollution dispersion: a review. In *New tools in turbulence modelling*, pages 265–280. Springer, 1996.

[17] H. Schmidt and U. Schumann. Coherent structure of the convective boundary layer derived from large-eddy simulations. *J. Fluid Mech.*, 200:511–562, 1989.

[18] E.D. Skyllingstad. Large-eddy simulation of katabatic flows. *Boundary Layer Meteor.*, 106:217–243, 2003.

[19] C.M. Smith and E.D. Skyllingstad. Numerical simulation of katabatic flow with changing slope angle. *Monthly Weath. Rev.*, 133:3065–3080, 2005.